Geophysical Research Letters

Supporting Information for

Intraseasonal sea level variability along the western coast of India in an eddy-resolving ocean general circulation model

Y. Yamagami[1], T. Suzuki[1], and H. Tatebe[1]

[1] Japan Agency for Marine-Earth Science and Technology, Yokohama, Japan

Contents of this file

Text S1 to S3

Figures S1 to S9

Introduction

This document contains supplementary documents and figures referred to in the main article.

Text S1

Model validation

We provide a brief validation of the COCO-HR model. When compared to observational data, COCO-HR simulations effectively reproduce the mean thermal and mechanical fields in the Indian Ocean. Model biases in SST are reduced in COCO-HR (Fig. S1). The model also realistically simulates key features of the mean circulation in the Indian Ocean, such as Indonesian Throughflow (12.2 ± 2.9 Sv compared to about 13 Sv in observations; Gordon et al., 2010) and the Mozambique Channel flow (16.3 ± 5.6 Sv compared to about 16.7 ± 8.9 Sv in observations; Ridderinkhof et al., 2010). In addition, tropical equatorial stratification is also realistically reproduced in COCO-HR, showing slight improvements compared to COCO-LR (Fig. S2). The seasonal cycle in the tropical Indian Ocean, which is characterized by semiannual surface velocity variations known as the Wyrtki jet (Yoshida, 1959; Wyrtki, 1973), was also reproduced in both COCO-HR and COCO-LR (Fig. S3). The zonal surface velocities in both models are smaller compared to those derived from drifters, with COCO-HR exhibiting a slight improvement in this bias. This result suggests that the basin-wide resonance between forced and reflected equatorial waves might be captured in these models (Han et al., 2011).

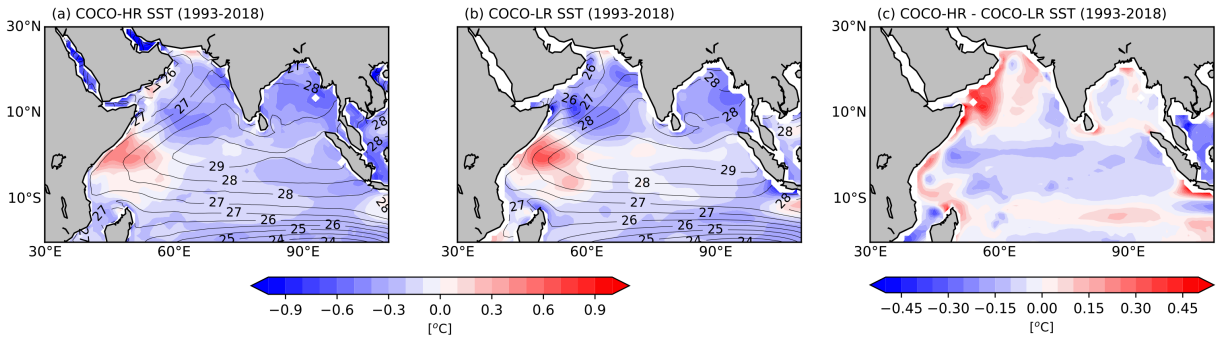

Figure S1. Sea surface temperature (SST) biases compared to PCMDI-SST for (a) COCO-HR and (b) COCO-LR for the period 1993-2018. Contours indicate the climatology in the models. (c) Difference in SST between COCO-HR and COCO-LR.

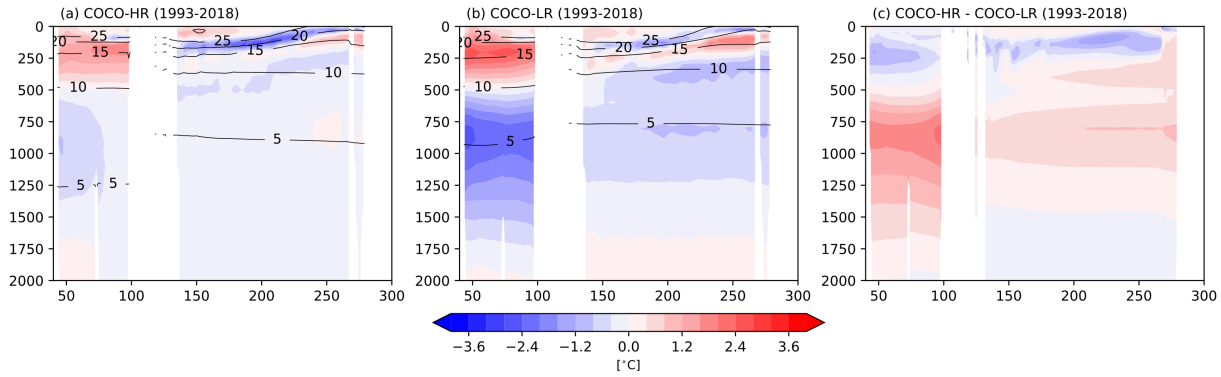

Figure S2. Temperature biases to WOA13v2 along the equator for (a) COCO-HR and (b) COCO-LR during the period 1993-2018 in the Indo-Pacific Ocean. The vertical axis represents depth [m] and contours indicate the climatology in the models. (c) Difference in temperature between COCO-HR and COCO-LR.

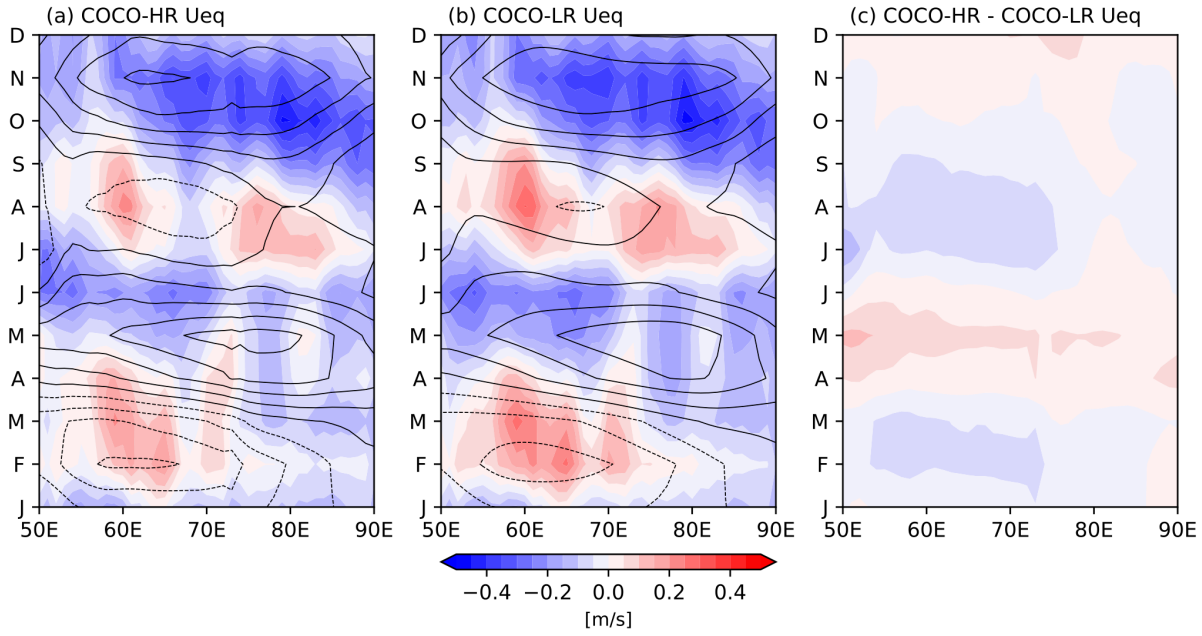

Figure S3. Zonal surface velocity bias along the equator (2.5°S-2.5°N) to the drifter-derived observation (Laurindo et al., 2017) for (a) COCO-HR and (b) COCO-LR during the period 1993-2018. Shaded areas show the difference from observations, and contours indicate the climatology for each model with 0.1 m/s intervals. The vertical axis indicates the seasonal progression, while the horizontal axis indicates longitude. (c) As in (a), but for the difference between COCO-HR and COCO-LR.

Text S2

Seasonal variations in SLAs for COCO-HR and COCO-LR

According to observations, the seasonal variations peak during winter (January) and reach their lowest in summer (August) (Fig. S4). The seasonal variations in COCO-HR closely align with the observations, with slight differences in the timing of the minimum. On the other hand, COCO-LR shows that the peak maximum occurs in April, and significantly underestimates the amplitude during winter, suggesting a lack of the key physical processes that explain these seasonal variations. Since the seasonal SLA variations are primarily driven by wind forcing over the southern tip of Sri Lanka, the Bay of Bengal, and the equator (Suresh et al., 2016), these results imply that COCO-LR may underestimate the adjustments by coastal Kelvin waves along the western coast of India.

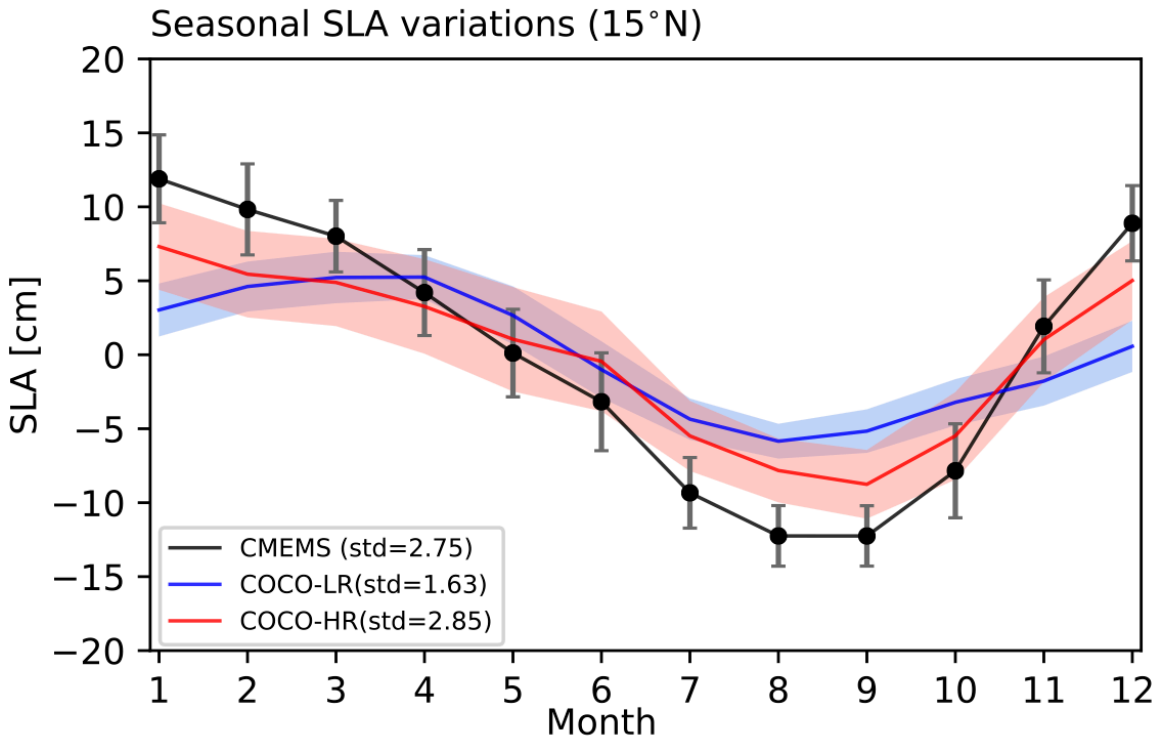

Figure S4. Seasonal variations in SLAs [cm] along the western coast of India (15°N; black boxes in Fig. 1) for the observations (CMEMS; black line), COCO-LR (blue line), and COCO-HR (red line). Bars and shaded areas indicate ±1 standard deviation. The annual mean has been subtracted from each time series to highlight the seasonal variations.

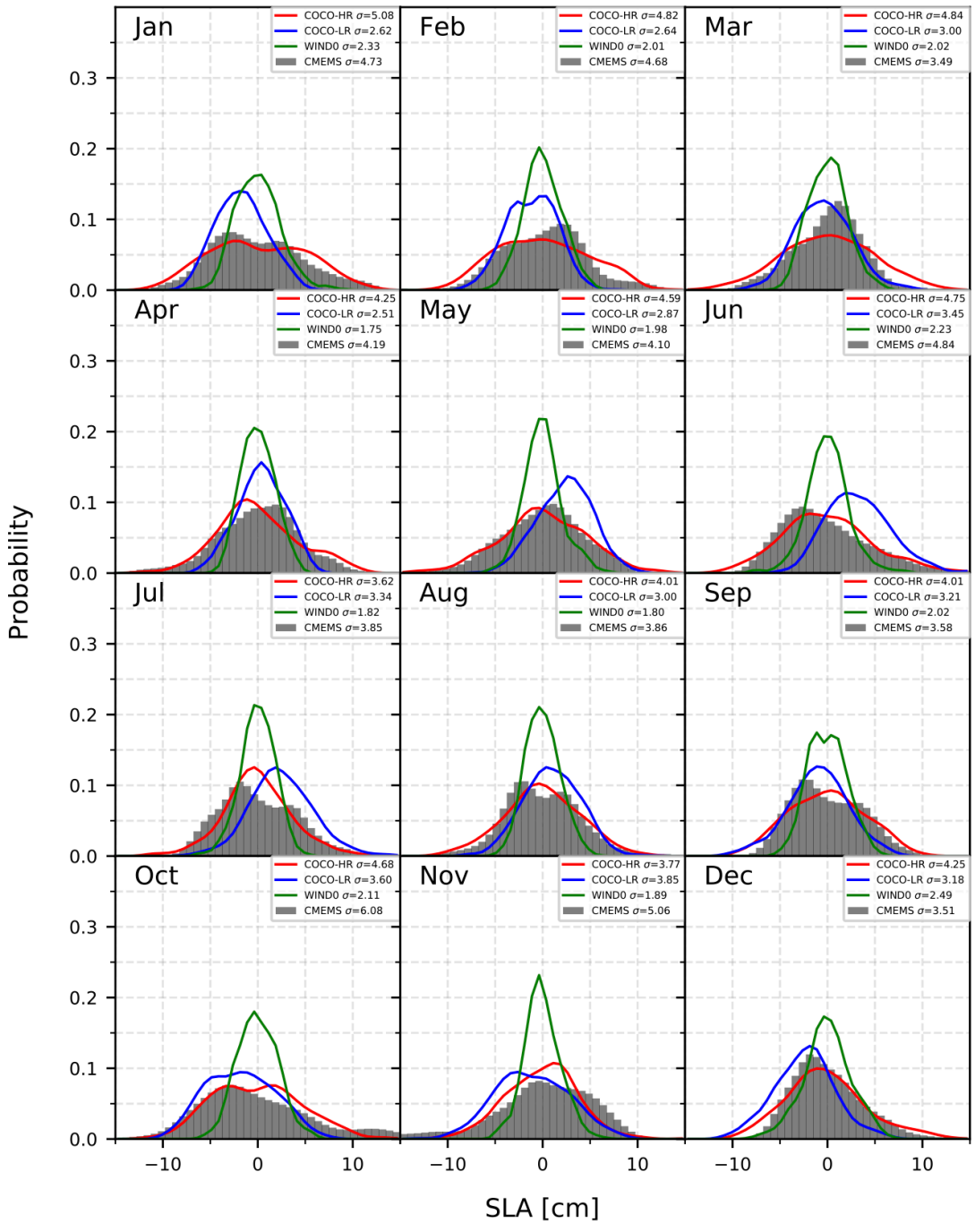

Figure S5. As in Figure 2, but for detrended SLAs without applying a bandpass filter.

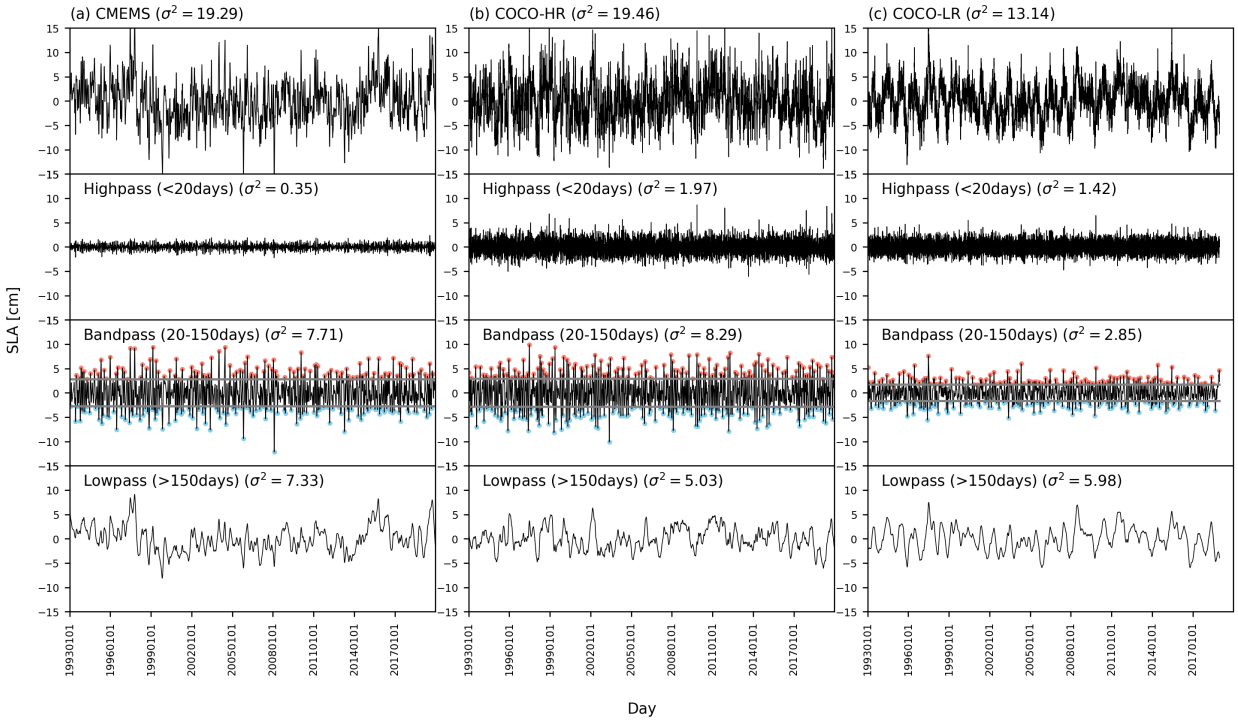

Figure S6. Variations in SLAs [cm] along the western coast of India (15°N; black boxes in Fig. 1) for (a) observations (CMEMS), (b) COCO-HR (blue line), and (c) COCO-LR. Top panels show detrended daily anomalies, while lower panels show the time series filtered into three frequency bands: high-pass (shorter than 20 days), band-pass (20-150 days), and low-pass (longer than 150 days). The variance for timeseries is shown in each panel.

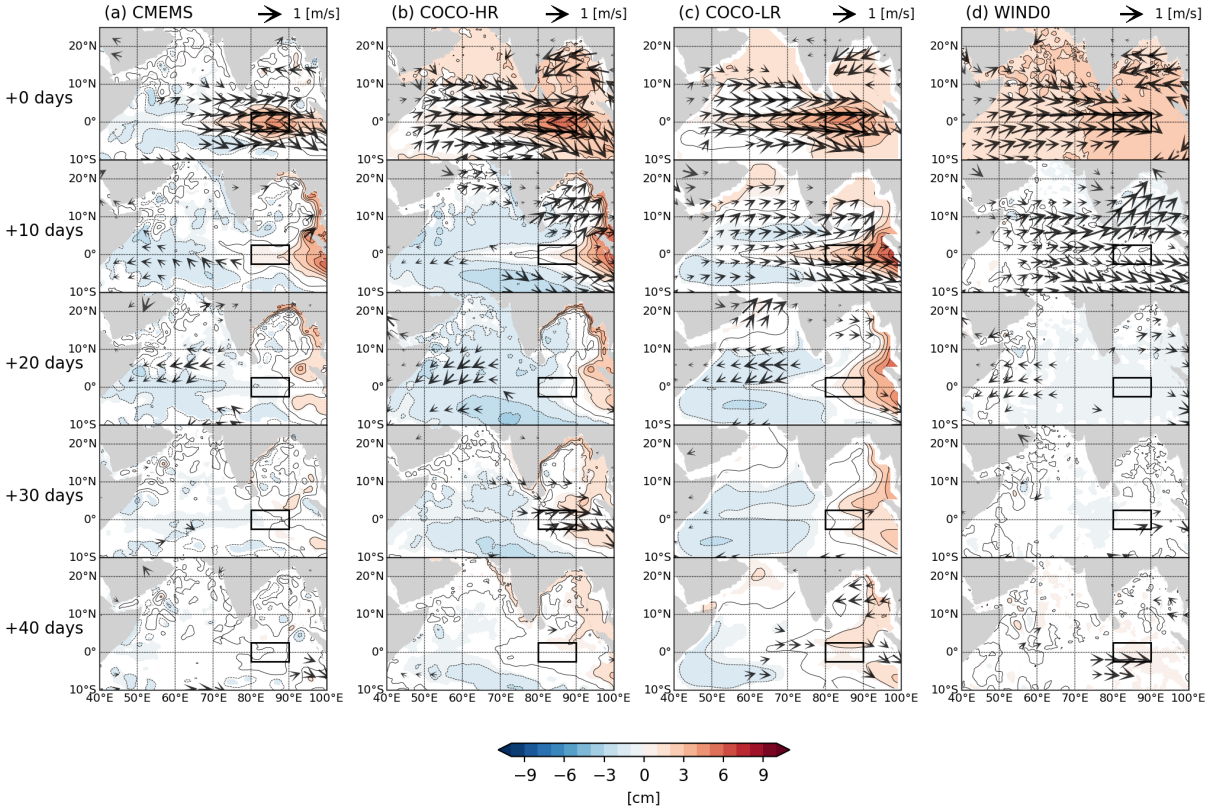

Figure S7. As in Figure 3, but for lag-composites for area-averaged SLA timeseries in the equatorial Indian Ocean (80°-90°E, 5°S-5°N; black boxes).

Text S3

Sufficient resolution for simulating coastal Kelvin waves

In this section, to examine the resolution dependency on representing coastal Kelvin waves, the model horizontal resolution is compared to the simulated Rossby deformation radius. Internal coastal Kelvin waves have a typical spatial scale of the Rossby deformation radius (e.g., Gill, 1982). The phase speed (c_1) and deformation radius (λ_1) of the first mode of the baroclinic Rossby wave, under the WKB approximation, are defined as follows (Chelton et al., 1998):

$$c_1 \approx \frac{1}{\pi}\int_{-H}^{0} N(z)\, dz \quad (1),$$

$$\lambda_1 = \begin{cases} \dfrac{c_1}{|f(\vartheta)|} & if\ |\vartheta| \geq 5° \\ \left(\dfrac{c_1}{2\beta(\vartheta)}\right)^{1/2} & if\ |\vartheta| < 5° \end{cases} \quad (2).$$

Where H is the depth of the ocean, $N(z)$ is the buoyancy frequency, ϑ is latitude, $f(\vartheta)$ is the Coriolis parameter, and $\beta(\vartheta)$ is the meridional gradient of $f(\vartheta)$. Figure S8 shows the estimated deformation radius for both COCO-HR and COCO-LR models. Both models have similar c_1 throughout the North Indian Ocean because of the similar stratification structure. However, since only COCO-HR can resolve continental shelves and steep ridges, the values differ around the atolls of the Maldives, in coastal areas of the Bay of Bengal, and along the western coast of India.

When comparing the nominal resolution of COCO-HR (COCO-LR), defined as $\Delta x = 0.1°$ (1.0°), with the deformation radius, there is a significant difference between the two. In COCO-HR, the resolution is sufficient (i.e., $\lambda_1 > 2\Delta x$) throughout the North Indian Ocean, except over the shallow continental shelf region, suggesting that COCO-HR is sufficient to represent coastal Kelvin waves. However, COCO-LR satisfies $\lambda_1 > 2\Delta x$ only in the equatorial regions, suggesting that the model lacks sufficient resolution in the North Indian Ocean.

We note that the comparison between deformation radius and resolution provides only a rough estimate. This is because rapid variations in $N(z)$ due to mixed layers in the upper ocean can introduce errors in the estimation of c_1 under the WKB approximation (Chelton et al., 1998). It is also important to note that SLA propagation from the equator

may be transformed into continental shelf waves, and local dynamics such as local coastal winds, instability, and river runoff can interrupt this propagation. However, previous studies have shown that coastal Kelvin waves are a key factor in explaining SLA variations along the western coast of India (e.g., Suresh et al., 2013). This suggests that the ability of COCO-HR to resolve coastal Kelvin waves contributes significantly to its reasonable representation of extreme SLA variations in this region.

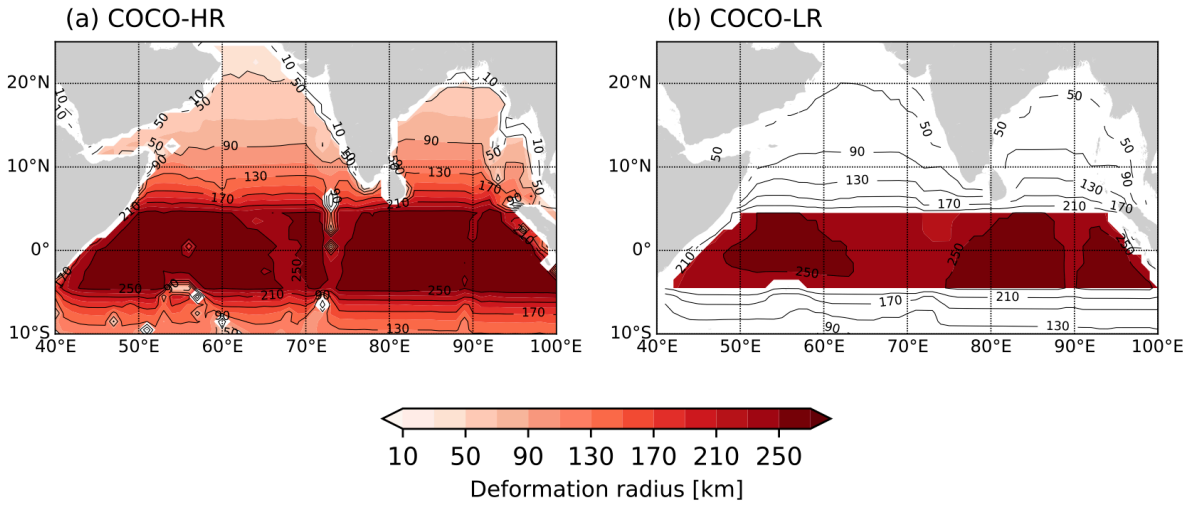

Figure S8. Deformation radius (λ_1) of the first mode of the baroclinic Rossby wave (Eq. 2) for (a) COCO-HR and (b) COCO-LR. The color indicates the area where the nominal horizontal resolution (Δx) is finer than the deformation radius (i.e., $\lambda_1 > 2\Delta x$).

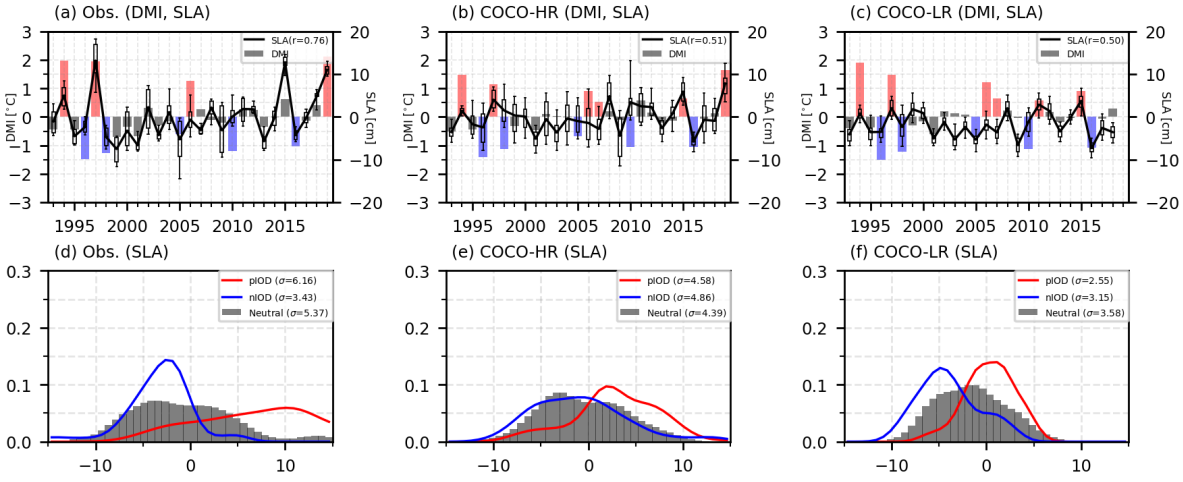

Figure S9. As for Figure 4, but for SLA timeseries without applying a bandpass filter.